DOI: 10.61782/fa.2023.0636

forum acusticum 2023

CORRESPONDENCE BETWEEN REFLECTED AND INCIDENT PULSE SIGNALS ON ACOUSTIC DIFFUSE SURFACES

Daniel F. P. Pazos[1*]

[1] Inmetro - Brazilian National Institute of Metrology, Duque de Caxias – RJ, Brazil

ABSTRACT

The reflection coefficient of acoustic diffuse surfaces shows at high frequencies unreasonable values greater than unity due to the promoted sound scattering. Aiming an adequate assessment of the reflection of such surfaces, it is proposed to quantify the correspondence (i.e. the similarity) between reflected and incident signals of impulse responses from diffusers. The product between a (specular or scattered) reflected pulse and a synchronized and weighted incident pulse, acquired without surface, results in a mutual correspondence signal. This measure is normalized by the square of this adjusted incident pulse, a standard auto-correspondence signal. In principle, the ratio between the spectral amplitudes of the resulting signals provides a corresponding reflection factor, which indicates the correspondence between the reflected and the incident sound pressure synchronized pulses. Analyses are done from measurements of normal incidence on samples of corrugated diffuse surfaces, including different incidence regions, besides a flat surface. It is shown that for diffuse surfaces, unlike the reflection coefficient, the proposed factor supplies good values along all over the spectrum. These results suggest the possibility of applying this parameter for the evaluation of sound reflection and diffusion of such surfaces.

Keywords: *sound reflection, sound scattering, diffusers, signal similarity.*

[*] ***Corresponding author***: *dfpazos@inmetro.gov.br*

1. INTRODUCTION

Diffuse surfaces are applied indoors as well as outdoors, aiming to promote scattering of the incident sound. Diffusion mitigates specular reflection by allowing sound to be reflected to other directions. The phenomenon is more remarkable at high frequencies, as the wavelengths are comparable to the dimensions of the surface irregularities. These can be corrugations, i.e. tops and recesses, or acoustic impedance discontinuities along the surface. Characterizing the sound reflection and scattering promoted by this type of surfaces is therefore important to optimize them.

To assess the sound reflection from surfaces in general, many parameters are available, such as the reflection coefficient (R), the ratio between the spectra of the reflected and the incident sound pressure. As a basic premise, the magnitude of R shall not exceed 1, once the reflected energy cannot physically be greater than the incident one. This measure can be experimentally obtained in laboratory or in-situ, by standard or non-standard methods [1]. Other related parameters are the sound absorption coefficient, the surface impedance, as well as the transfer function between measurements with and without surface and the reflection index (a.k.a. reflectance), the ratio between the reflected and the incident energy. Since the characterization of scattering is not so simple [2], researches continue to be conducted in order to experimentally evaluate the sound reflection from diffuse surfaces.

Recently, investigations on the sound reflection from corrugated diffuse surfaces have been done with a two-microphone method [3]. Impulse responses were measured at two positions close to samples of periodic corrugated surfaces under normal incidence. Each measured signal contains incident pulses followed by reflected ones, whose time-delays depend on the measuring positions. The method consists in alternately time matching (synchronizing) the incident or the specular reflected pulses

of a measuring position to their corresponding pairs of the other position, taking into account their amplitude weighting, in order to be subtracted and eliminated from each other. Two signals with inverted pulses are obtained, one ideally composed only by the incident pulses and the other only by the reflected ones. Both resulting signals are suitably synchronized and amplitude weighted to obtain the reflection coefficient of the surfaces. Although well applied for flat surfaces, for diffuse ones there are scattered pulses beyond the specular part, causing the energy of the measured reflected signal to be greater than that of the incident pulse. Thus, values of the reflection coefficient greater than unity are obtained at high frequencies [3].

By using impulse responses to determine the reflection coefficient of diffuse surfaces, the reflected pulses could be selected and compared with their respective originating incident pulses. This was investigated in [3], applying a very short time window to separate the specular pulses from the delayed scattered ones. However, since usually the reflected pulses come very close to each other, it is unfeasible through this technique to adequately eliminate the scattered pulses, as there is a commitment between the size of the window and the quality of the results. A very short and steep window leads to lose resolution of the reflection coefficient, mainly at low frequencies, besides introducing spurious spectral components. On the other hand, with a wider and smoother window, it is impossible to effectively attenuate the scattered pulses, thus remaining the problem of the reflection coefficient at high frequencies, which contains many oscillations, due to the interference between the reflected pulses (comb filter effect) [3].

As proposed in [4, 5], for a more suitable assessment, it would be necessary to measure at more positions on the surface (multi-microphone method), so that it could be obtained different reflection coefficients, related to the further orders of reflection, besides the specular one. However, it is a rather complex method and may require many measurement points close to the surfaces.

In view of these limitations for the reflection coefficient of diffuse surfaces, other approaches may be elaborated. This work proposes to quantify the similarity between reflected and incidence pulse signals on such surfaces. Since it is about the relation between the originating incident and corresponding reflected pulses, herein signal similarity is also called correspondence. One way to identify the similarity between overlapping pulses is by the product between them. So, after pulse synchronization and amplitude weighting, it is carried out the multiplication between reflected and incident signals, besides the incident by itself, obtained from impulse responses under normal incidence with and without diffuse surfaces. The product between synchronized pulse signals results in a combo-signal of the corresponding (matching) pulses, eliminating the non-corresponding ones. The ratio between the spectral amplitudes of the resulting signals is a parameter that allows quantifying the mutual correspondence between the reflected and the incident signals. It is possible to evaluate not only the specular reflection from the region of normal incidence, but also the scattered reflection from adjacent regions, being only necessary to obtain the incident pulses on such regions. Analyzes of the experimentally determined parameter with periodic corrugated (rough) surfaces of square and triangular profiles, in addition to a flat profile are done. Such parameter may be useful for the evaluation of the scattering and reflection of diffuse surfaces.

2. CORRESPONDENCE BETWEEN SIGNALS

Similarity (or correspondence) between signals is a characteristic that indicates how much a signal is related to another one, being the cross-correlation and the dot product ways of mathematically representing it. Considering two signals at time t, $s_a(t)$ and $s_b(t)$, which the *related signal*, $s_b(t)$, is to be linearly described over a specific time interval by the *standard (or model) signal*, $s_a(t)$. This relation could be done through a single constant correspondence (or corresponding) factor $F_{b,a}$ between them, so that $s_b(t) \approx F_{b,a}\, s_a(t)$. So, the error ε in this approximation at t is $\varepsilon_{b,a}(t) = s_b(t) - F_{b,a}\, s_a(t)$. The best value of $F_{b,a}$, for such approximation between t_1 and t_2, can be estimated by the one which minimizes the mean square error over this interval [6], which is

$$\left.\overline{\varepsilon_{b,a}^2}\right|_1^2 = \frac{1}{t_2 - t_1}\int_{t_1}^{t_2}\left[s_b^2 - 2s_b F_{b,a} s_a + F_{b,a}^2 s_a^2\right]dt \qquad (1)$$

This condition can be obtained from the null derivative of $\overline{\varepsilon_{b,a}^2}$ with respect to $F_{b,a}$, leading to

$$\int_{t_1}^{t_2}\left[\frac{\partial s_b^2}{\partial F_{b,a}} - \frac{\partial\left(2s_b F_{b,a} s_a\right)}{\partial F_{b,a}} + \frac{\partial\left(F_{b,a}^2 s_a^2\right)}{\partial F_{b,a}}\right]dt = 0 \qquad (2)$$

Once $s_a(t)$ and $s_b(t)$ do not depend on $F_{b,a}$, their derivatives are zero and one gets the expression [7]

$$\left.F_{b,a}\right|_1^2 = \frac{\int_{t_1}^{t_2} s_b s_a dt}{\int_{t_1}^{t_2} s_a^2 dt} \qquad (3)$$

Therefore over a given time interval the optimal corresponding factor $F_{b,a}$ between the related and the standard signal can be expressed by the ratio between the dot product (zero lagged cross-correlation) of these signals and the energy (zero lagged autocorrelation) of the standard signal.
So if the time interval turns infinitesimal, the instantaneous correspondence factor ($F_{b,a,t}$) for any instant t can be given by the ratio between the integrands of the expression above. Although simply dividing the related signal by the standard one also results in the instantaneous relation between them, the product of signals indicates the overlap intensity and similarity over time. This creates a mutual *correspondence signal*, which is compared through division to the square of the standard signal, an auto-correspondence signal and a pattern of energy distribution over time. If $|s_b(t)| \leq |s_a(t)|$, it is obtained $|F_{b,a,t}| \leq 1$.

2.1 Correspondence factor in frequency

Analogously in the frequency domain, the ratio between the spectral amplitudes of the product of signals and the square of the standard signal provides the *correspondence factor for a given frequency f* ($F_{b,a}(f)$). From the convolution theorem, the Fourier transform (FT) of the product of two signals in time results in a convolution operation (*) between the spectra of each signal [6]. The convolution generates a *correspondence spectrum* ($C_{a*b}(f)$), which expands the spectra of the signals and indicates the similarity between them in frequency. The autoconvolution of the standard spectrum ($C_{a*a}(f)$) refers to the pattern of spectral similarity and normalizes the correspondence spectrum between the signals, through division. So, being $S_a(f)$ and $S_b(f)$ the spectra of $s_a(t)$ and $s_b(t)$ respectively, the following expression is obtained

$$F_{b,a}(f) = \frac{\mathrm{FT}[s_b s_a]}{\mathrm{FT}[s_a^2]} = \frac{S_b(f) * S_a(f)}{S_a(f) * S_a(f)} = \frac{C_{b*a}(f)}{C_{a*a}(f)} \qquad (4)$$

2.2 Correspondence Factor between reflected and incident sound pulse signals

Let's now consider an impulsive sound wavefront reaching a wide reflecting surface, over which the sound pressure is measured at a point above a surface region subjected to normal incidence (Fig. 1 above left). The measured time signal $p(t)$ consists first of a direct or incident part $p_{i,0}(t)$ at time $t_{i,0}$, referring to the pulse that impinges on the surface at such region, and a reflected part $p_r(t)$. This is composed by the specular or 0th-order reflected pulse, occurring at the subsequent time t_0 and, in the case of non-divergent diffuse surfaces, normally followed by several scattered pulses, each one at a given time t_n, (being $n = 1, 2, \ldots, N$ the order of reflection) (Fig. 1 above right). The earlier specular reflected pulse is originated from the normally incident one, exhibiting, providing the case of a flat and reflecting surface, great correspondence or similarity with it. Additionally for diffuse surfaces, the scattered pulses are due to the oblique incident pulses of the wavefront, which reach adjacent regions to the normal incident one, diffusely reflected, thus arriving latter (Fig. 1). Then, expressing each pulse as a triangular function $\Delta(t)$, occurring at t_n, with very narrow time width δt_n (so that $\delta t_n << t_n$) and amplitude A_n, the incident and reflected part of the measured signal ($p(t) = p_{i,0}(t) + p_r(t)$) can be represented respectively by

$$p_{i,0}(t) = A_{i,0}\Delta\left((t - t_{i,0})/(\delta t_{i,0}/2)\right) \qquad (5)$$

$$p_r(t) = \sum_{n=0}^{N} A_n \Delta\left((t - t_n)/(\delta t_n/2)\right) \qquad (6)$$

To overcome the problem in evaluating the sound reflection from diffuse surfaces by the reflection coefficient, the study of the correspondence between signals [7] can be considered. For impulsive signals, cross-correlating the incident and the reflected signals tends to accuse correspondence to any reflected, specular or scattered pulse, even if it does not stem from the measured incident one, as cross-correlation does not necessarily imply causality.
On the other hand, the product of signals indicates the instantaneous correspondence between them, since for more time overlapping, the greater it will be at a given instant. Furthermore, the product of impulsive signals imposes certain causality through pulses orthogonality, enhancing the most synchronous ones and suppressing non-overlapping pulses, since the amplitude of one of them is zero or very small.
So let $p'_{i,0}(t) = A'_{i,0}\Delta((t - t_{i,0})/(\delta t_{i,0}/2))$ be the incident signal (Fig.1 below left), after synchronization (displaced from interval $t_0 - t_{i,0}$) and amplitude weighting as $A'_{i,0}$ (due to geometrical spreading) with the specular pulse of the reflected signal, which is $p_{r,0}(t) = A_0\Delta((t - t_0)/(\delta t_0/2))$. The product of the reflected signal (related signal) and the synchronized and weighted incident (standard signal) results in the correspondence signal (Fig. 1 below right), which is given theoretically only by the product of the reflected and the incident pulses

$$p_r(t)p'_{i,0}(t) = A_0 A'_{i,0}\,\Delta\left(\frac{t - t_0}{(\delta t_0/2)}\right)\Delta\left(\frac{t - t_{i,0}}{(\delta t_{i,0}/2)}\right) \qquad (7)$$

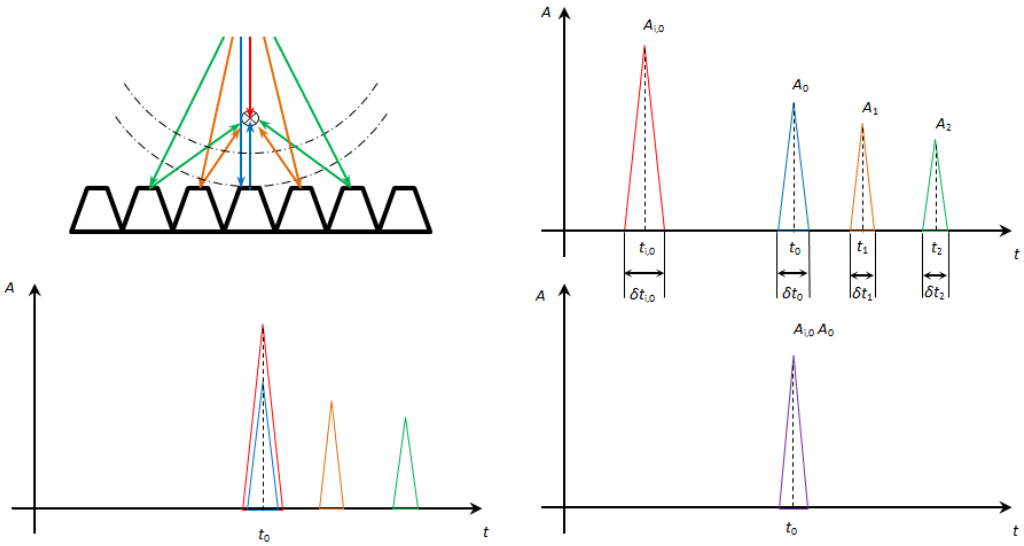

Figure 1. Corrugated surface under incident wavefront, showing the incident and reflected pulse paths (above left). Impulse response: incident and reflected pulses (above right). Incident pulse synchronized to the specular one (below left). Correspondence signal (below right).

Therefore, assuming that there is no overlap between the scattered and the incident pulses, a combined pulse signal between the specular reflected and incident pulses is obtained, eliminating the subsequent and non-corresponding ones. To normalize this correspondence signal, it is compared to the square of the synchronized and amplitude weighted incident signal, a standard energy distribution over time, i.e., $p'^2_{i,0}(t) = A'^2_{i,0}\Delta^2((t-t_0)/(\delta t_{i,0}/2))$. So, being $P'_{i,0}(f)$ and $P_r(f)$ the spectra of $p'_{i,0}(t)$ and $p_r(t)$ respectively, a normalized measure of the correspondence between these signals in frequency is given by the ratio between the convolution of the reflected and the incident spectra ($C'_{r*i,0}(f)$) and the autoconvolution of the incident one ($C'_{i,0*i,0}(f)$)

$$F_{r,i,0}(f) = \frac{\mathrm{FT}\left[p_r(t)p'_{i,0}(t)\right]}{\mathrm{FT}\left[p'^2_{i,0}(t)\right]} = \frac{P_r(f) * P'_{i,0}(f)}{P'_{i,0}(f) * P'_{i,0}(f)}$$

$$F_{r,i,0}(f) = \frac{C'_{r*i,0}(f)}{C'_{i,0*i,0}(f)} \qquad (8)$$

This ratio is herein called as the (0 order) *corresponding reflection factor* ($F_{r,i,0}(f)$), a dimensionless parameter to evaluate in frequency in how much the specular reflected pulse signal is related to the originating synchronized incident one. As the amplitude of any simple reflected pulse (i.e., no overlapping with any other) shall be equal or less than that of the incident one, $|F_{r,i,0}(f)| \leq 1$. In addition, similar n order parameters ($F_{r,i,n}(f)$), referring to the n order scattered reflections due to incident pulses ($p_{i,n}(t)$) on adjacent regions can be determined, assuming that there is no overlap between the scattered n order reflection pulses ($p_{r,n}(t)$).

3. EXPERIMENTAL SETUP

The proposed parameter was experimentally determined with data obtained from measurements on samples of periodic corrugated surfaces (Fig. 2.a), a square profile and a triangular one, besides a flat surface (Fig. 2.b). They were made of thin wooden panels with rectangular dimensions (2.10 m x 1.48 m) (Fig. 2.a). On one face of each sample, 21 ribs 1.48 m long were parallelly and periodically spaced, forming corrugated profiles along the largest side of the panels. The corrugations featured period $\Lambda = 10$ cm, height $H = 5.5$ cm, width $b = 5$ cm for the square profile and base $b = 10$ cm for the triangular one (Fig. 2.d). The opposite face to each corrugated profile is a flat surface, on which measurements were also carried out, by turning the samples over. The entire surfaces were covered by laminated plastic, in order to promote good sound reflection.

Each sample was separately laid on the floor of a laboratory chamber large enough and far from any obstacles, so that spurious reflections would not contaminate the signal parts of interest and could be easily eliminated. Normal incidence

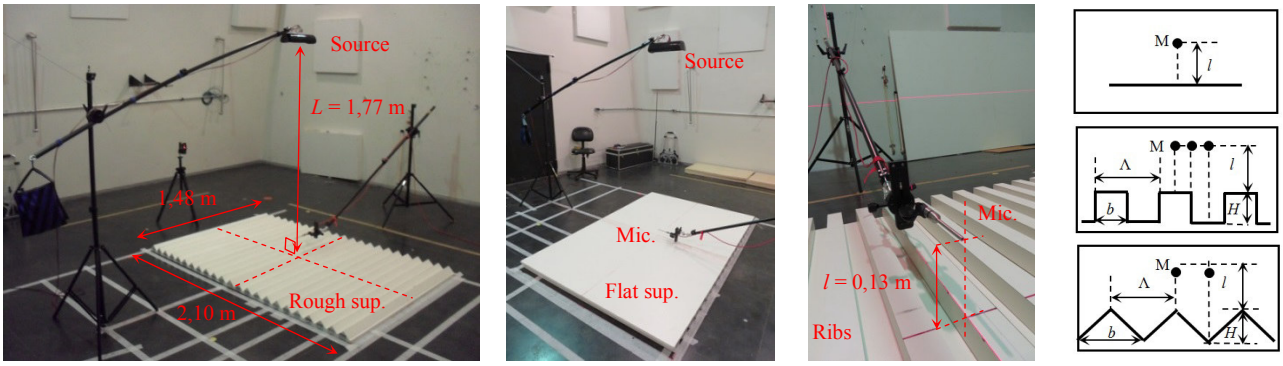

Figure 2. Surfaces and dimensional parameters: corrugated (a) and flat (b). Microphone over a mid recess (c) and measurement positions (d): flat (above), square profile (middle) and triangular profile (below).

impulse responses were measured with a ¼" microphone placed at $l = 13$ cm over the central region of the samples (Fig. 2.c). For the corrugated samples, the microphone was mounted on a rib (top), but also on a top corner and on an adjacent recess (Fig. 2.d). A directional sound source over the central region of the surfaces at a distance of $L = 1.77$ m was aligned to the microphone, for normal incidence, emitting a short sweep signal, flat enough between a 100 Hz and 10 kHz frequency range, in order to obtain good impulse responses (Fig. 2.a and Fig. 2.b). Preliminary measurements allow considering spherical wave propagation for the source-microphone distance. The excitations and measurements were controlled and processed by a signal analysis software.

In order to obtain incident pulses free from reflections, measurements without samples and far from any surface were also performed. In addition to measuring the free normal incidence at $L' = 1.75$ m from the source, adjacent oblique incident pulse signals were also obtained, due to the directionality of the source. For this purpose, the microphone was moved perpendicularly to the central axis of the source, along the direction of the surfaces corrugations, performing measurements without sample on different positions adjacent to this axis. The incident pulses can be properly synchronized and weighted to the specular and scattered reflected ones, in order to obtain $F_{r,i,n}(f)$.

4. RESULTS

Measurement results are hereafter presented. Fig. 3.a shows the time records of the reflected parts $p_r(t)$ from the flat ($p_{r,f}(t)$), square ($p_{r,q}(t)$) and triangular ($p_{r,t}(t)$) profiles, measured on the center of the samples (on the corrugated surfaces over the mid rib). The amplitude unit is arbitrary, since dimensionless parameters are to be obtained. For the flat surface, the reflection contains only the specular pulses, occurring at $t_0 = 5.50$ ms ($(=(L+l)/c$, where $c = 346$ m/s is the speed of sound). On the other hand, besides specular pulses with smaller amplitude, for the corrugated profiles, scattered pulses are observed, which are considerably larger for the triangular one. It is also plotted the normal incident signal, $p'_{i,0}(t)$, obtained without sample, synchronized and amplitude weighted to the first specular reflected pulse at t_0, multiplying it by $t'_{i,0}/t_0 = 0.92$ ($t'_{i,0} = 5{,}1$ ms $= L'/c$) to compensate the geometric decay by spherical propagation. This incident signal was also used to eliminate through subtraction the incident part of the impulse responses at $t_{i,0} = 4{,}77$ ms ($=(L-l)/c$) obtained with samples. Since there are intrinsic imperfections in this procedure, remaining traces are observed at $t_{i,0}$ in the reflection records.

The superposed incident signal, $p'_{i,0}(t)$, is then multiplied by each of these reflected signals, in addition by itself, obtaining the correspondence signals and the square of the incident one, shown in Fig. 3.b Again, the amplitude dimension is arbitrary. This way, the specular pulses are selected and the scattered ones attenuated, indicating the instants and intensity of correspondence between the incidence and the reflection signals. It can be seen that the reflection specular pulses from the flat profile are very similar to the incident one, while those from the square profile features some correspondence and those from the triangular one almost none, since in this case the central top is a rib edge with a tiny surface for specular reflection from the normal incident pulse. Moreover, the subtractions remnants of the incident part in the reflection signals were suppressed with this multiplication operation, because

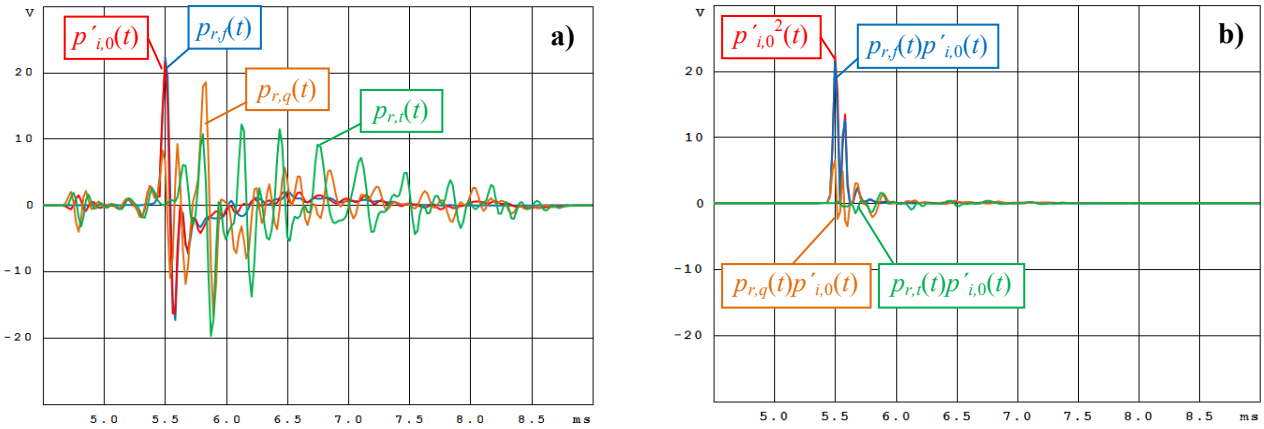

Figure 3.a) Signals $p'_{i,0}(t)$ (red), $p_{r,f}(t)$ (blue), $p_{r,q}(t)$ (ocher) and $p_{r,t}(t)$ (green);
b) Corresp. signals $p'^2_{i,0}(t)$ (red), $p_{r,f}(t)p'_{i,0}(t)$ (blue), $p_{r,q}(t)p'_{i,0}(t)$ (ochre) and $p_{r,t}(t)p'_{i,0}(t)$ (green).

$p'_{i,0}(t)$ shows almost zero amplitude before the occurrence of the respective pulses. On the other hand, although there is good attenuation of scattered pulses in the reflected signals from diffuse surfaces, it can be observed that the suppression is not perfect and some residual traces still occur after the specular pulses, since the incident pulse features a time decay tail, which slightly overlaps the following scattered ones.

Applying adequate time windowing after the main pulses, late spurious reflections from other obstacles and from the corners of the samples, which can distort the results, are eliminated. This way in Fig. 4.a, it is plotted the spectra of the signals, between 100 Hz and 10 kHz, before multiplication by $p'_{i,0}(t)$. The scale is in decibels relative to the unitary effective amplitude. At lower frequencies the reflection spectra of the diffuse surfaces are somewhat similar to that of the flat one and also to the incident spectrum, but at higher frequencies they feature more energy and the comb-effect filter is observed due to the interference between the reflection peaks. The flat surface reflection spectrum also exhibits some small ripples along the spectrum, attributed to the remnants of the subtraction of the incident pulse.

In Fig. 4.b it is presented the correspondence spectra, after the product between the signals, i.e. the convolution between reflection and incidence spectra ($C'_{r*i,0}(f)$), besides the autoconvolution of the latest ($C'_{i,0*i,0}(f)$). Once the scattered components were quite removed, the correspondence spectra are smoother, always showing smaller magnitude than the autoconvolution spectrum of the

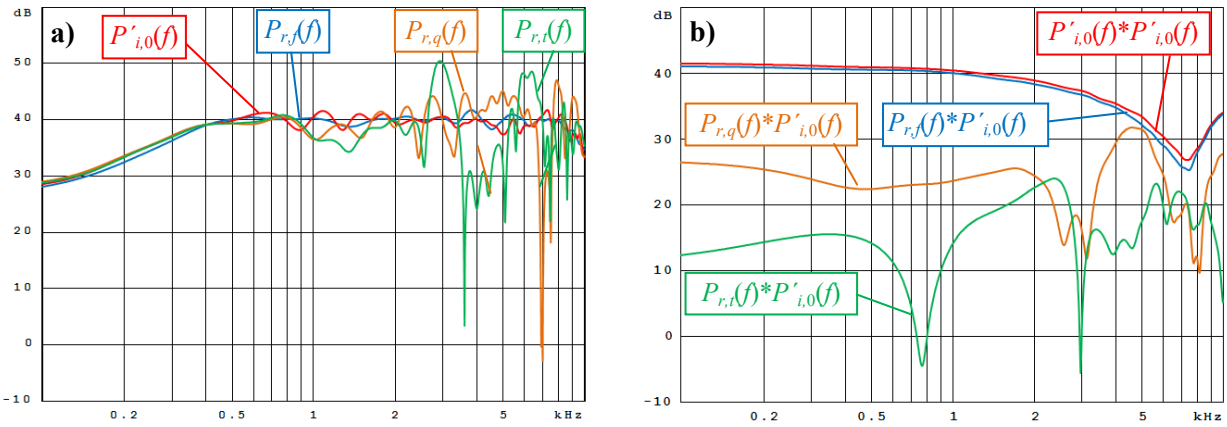

Figure 4.a) Spectra $P'_{i,0}(f)$ (red), $P_{r,f}(f)$ (blue), $P_{r,q}(f)$ (ochre) and $P_{r,t}(f)$ (green);
b) Corresp. spectra $C'_{i,0*i,0}(f)$ (red), $C'_{r,f*i,0}(f)$ (blue), $C'_{r,q*i,0}(f)$ (ochre) and $C'_{r,t*i,0}(f)$ (green).

incident signal, mainly for the triangular one. However, it is observed some comb filter effect due to the presence of spurious scattering peaks on the signals, which could not be completely removed by signals multiplication in time.

From these spectra, the reflection coefficients and the corresponding reflection factors were determined and compared to each other. This way in Figs. 5, these parameters are shown for the flat (Fig. 5.a: $R_f(f)$ and $F_{r,i,0,f}(f)$), the square (Fig. 5.b: $R_q(f)$ and $F_{r,i,0,q}(f)$) and the triangular profile (Fig. 5.c: $R_q(f)$ and $F_{r,i,0,t}(f)$).

Up to about 800 Hz, the first parameter ($R(f)$) shows values close to unity for all profiles, indicating high sound reflection. However, for higher frequencies it is observed oscillating and discrepant values already mentioned, especially for the corrugated profiles. On the other hand, the proposed parameter ($F_{r,i,0}(f)$) exhibits plausible values smaller than unity along all over the spectra, even at high frequencies, since the scattering pulses were almost fully eliminated through the product of signals. Furthermore, values of $F_{r,i,0}$ are much smaller for the corrugated profiles (averages around 0.3), mainly for the triangular one (Fig. 5.c), as expected. It is remarkable how the proposed parameter provides even better values for the flat surface (Fig. 5.a), considering that the remnants of the subtractions of the incident pulses were well suppressed by the product.

With the same reflection signals, corresponding reflection factors were also determined for scattered pulses of the 3rd reflection order ($F_{r,i,3}(f)$, Fig. 5.d) at $t_3 = 5{,}83$ ms ($\approx(L+2H+l)/c$), coming from the adjacent recesses to the middle rib of the corrugated profiles. Due to the symmetry of the profiles relative to the source-microphone axis, it is assumed that such scattered pulses are formed by two synchronized reflected signals, each one from an incident pulse on the adjacent recesses to the middle rib (Fig. 1

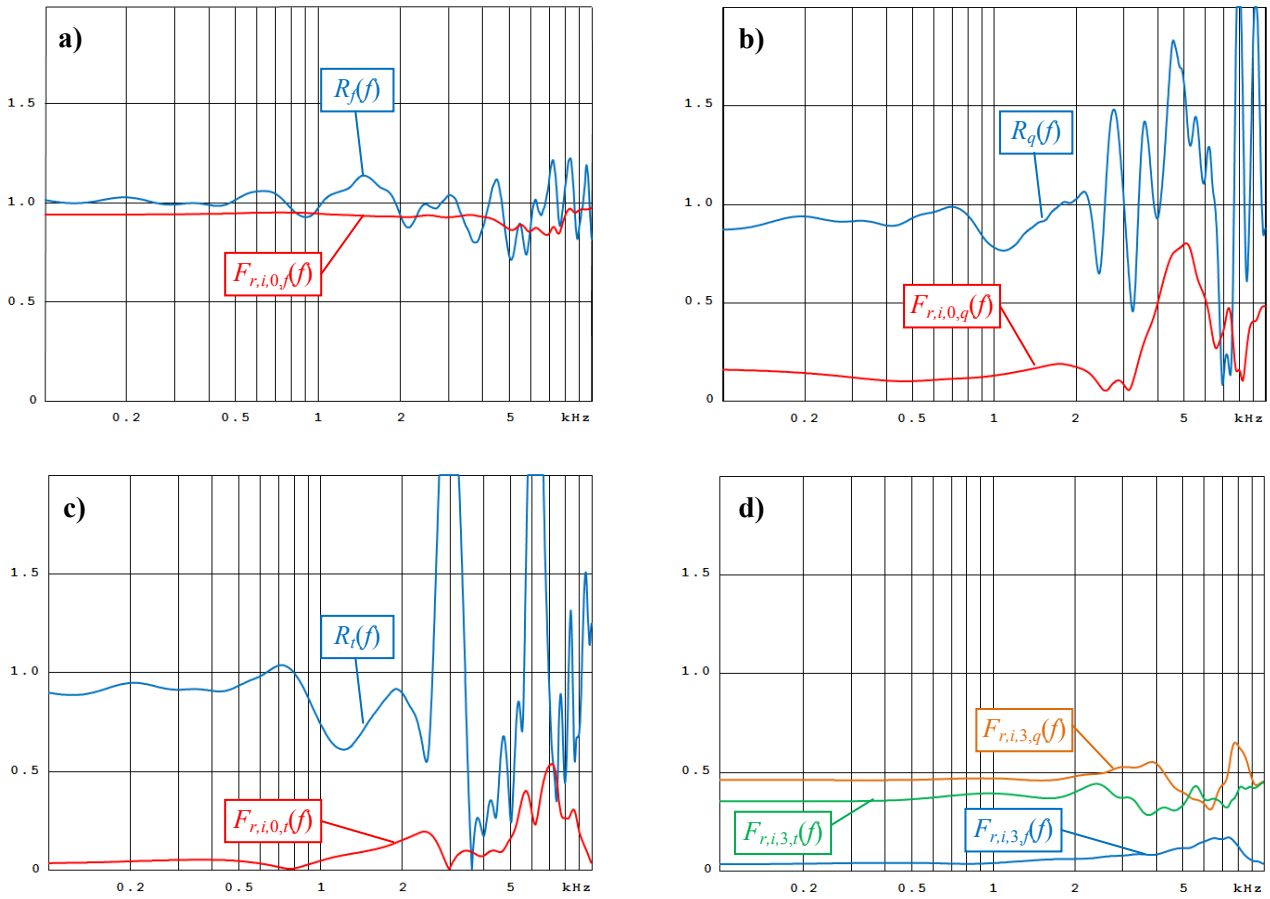

Figure 5. $R(f)$ (red) e $F_{r,i,0}(f)$ (blue) for the flat (a), square (b) and triangular profile (c), besides $F_{r,i,3}(f)$ (d) for the flat (blue), square (ocre) and triangular profiles (green).

above left). So, for the determination of $F_{r,i,3}(f)$, a pair of incident pulses were used, measured without sample on the right and on the left side of the central axis of the source ($p_{i,3,d}(t)$ and $p_{i,3,e}(t)$), synchronized and properly amplitude weighted, i.e. $p'_{i,3}(t) = p'_{i,3,d}(t) + p'_{i,3,e}(t)$. With these incident adjacent pulses at t_3, $F_{r,i,3}(f)$ was also determined for the flat sample, aiming to assess how this parameter responds when there is no synchrony between single reflected pulses and the incident one. As expected for the flat profile, due to the offset between the specular reflection and the adjacent incidence pulses, besides the absence of scattering, the parameter shows very small values along the spectrum, averaging about 0.10. However, in view of the decay tail of the specular reflection pulse, which slightly overlaps the incident one, values up to 0.17 occur around 7 kHz. On the other hand, for the corrugated profiles, due to the synchrony between the incident pulse and those scattered from the central recess, whose amplitudes are even greater than that of the specular pulse from the central rib, values of $F_{r,i,3}(f)$ are much higher than those of specular reflection $F_{r,i,0}(f)$ (Figs. 5.b and 5.c). This means that there is more correspondence for the reflected pulses from the adjacent recesses than from the specular reflection, averaging about 0.48 for the square profile and 0.38 for the triangular one.

5. CONCLUSIONS

The correspondence between reflected and incident sound pulse signals on diffuse surfaces seems to be an useful tool to be considered to evaluate the sound reflection of such surfaces. The proposed correspondence factor between these pulse signals, properly synchronized and amplitude weighted, is a metric that provides plausible and more easily interpreting values in relation to the usual reflection coefficient for diffuse surfaces. Even for flat surfaces, this parameter results in much better values, as the multiplication between impulsive signals vanishes unsynchronized residual parts of subtractions, which somewhat distort the reflection coefficient values.

Although the results of the analyzes with two types of corrugated profiles, in addition to a flat surface, have shown to be positive, there are still topics to be further investigated. For example, the issue that the incident signal is not a perfect impulse, featuring a decay tail which can overlap the unsynchronized scattered pulses. This can result in distortion of the results, i.e. some correspondence between the incident and the scattered pulses, even though the latest do not stem from the first. Thus, given a measured impulsive signal, it is to investigate how corrugations geometry or surface irregularities affect results distortion due to the overlapping between no corresponding pulses.

Another topic is about the results for incidence on different regions of diffuse surfaces, for example incidence not only on a top, but also on a recess. This way, to combine the results in a single value, an average of reflection signals from normal incidence on different surfaces regions could be cross-correlated with a weighted incident signal along the decay tail of the averaged specular reflection. Thus, it could be obtained a single corresponding factor relating the averaged specular reflection to the incidence on different regions of diffuse surfaces. These and other issues can be investigated and may contribute to the characterization of sound reflection and scattering from diffuse surfaces.

6. REFERENCES

[1] E. Brandão, A. Lenzi and S. Paul, "A Review of the in situ impedance and sound absorption measurement techniques," *Acta Acustica*, 101, pp. 443-463, 2015.

[2] M. Darmon, V. Dorval and F. Baqué: "Acoustic scattering models from rough surfaces: a brief review and recent advances," *Applied Sciences*, Vol. 10, Is. 22, 2020.

[3] D. Pazos and R. Musafir, "Medição da reflexão sonora de superfícies corrugadas com o método de dois microfones," in *Proc. of the XXVII Encontro da Sociedade Brasileira de Acústica – Sobrac*, (Brasília, Brazil), 2017.

[4] T. Wu, Y. Lam, and T. Cox, , "Measurement of non-uniform surface by the two microphone method," in *Proc. of the 17th International Congress on Acoustics – ICA*, (Rome, Italy), 2001.

[5] W. Lauriks, G. Jansens, L. De Geetere, et al., "Evaluation of free field techniques for the measurement of the surface impedance of sound absorbing materials," in *Proc. of the 17th International Congress on Acoustics – ICA*, (Rome, Italy), 2001.

[6] R. Higuti and C. Kitano: *Sinais e Sistemas*. V. 1.1, Ilha Solteira, Brazil: DEE-FEIS-UNESP, 2003. Av. at: https://www.feis.unesp.br/Home/departamentos/engenhariaeletrica/optoeletronica/sinais_e_sistemas.pdf

[7] Z. Sun, G. Wang, X. Su, et al., "Similarity and delay between two non-narrow-band time signals," *arXiv*, *Electrical Engineering and Systems Science - Signal Processing*, Cornell University, 2020. Av. at: https://arxiv.org/ftp/arxiv/papers/2005/2005.02579.pdf